Grafting luminescent metal-organic species into mesoporous MCM-41 silica from europium(III) tetramethylheptanedionate, $Eu(thd)_3$

A. Fernandes, J. Dexpert-Ghys, A. Gleizes, A. Galarneau and D. Brunel

Centre d'Elaboration de Matériaux et d'Etudes Structurales (UPR 8011), rue Jeanne Marvig, BP 4347, 31055 Toulouse cedex 4, France
Centre Interuniversitaire de Recherche et d'Ingénierie des Matériaux (UMR 5085), ENSIACET/INPT, 118 route de Narbonne, 31077 Toulouse cedex 4, France
Laboratoire des Matériaux Catalytiques et Catalyse en Chimie Organique (UMR 5618) CNRS/ENSCM/UM1 (Institut Gerhardt FR 1878), ENSCM, 8 rue de l'Ecole Normale, 34296 Montpellier cedex 5, France
Received 27 July 2004; revised 8 December 2004; accepted 14 December 2004. Available online 23 May 2005.

Abstract

Mixed systems with Eu(III) β-diketonates as optically active guest species, and mesoporous silicas MCM-41 as a host matrix have been investigated. The grafting of europium(III) onto the inner walls of unmodified MCM-41 has been achieved starting from $Eu(thd)_3$ (thd = 2,2,6,6-tetramethyl-3,5-heptanedionate), using two routes: wet impregnation (WI) at room temperature, and chemical vapour infiltration (CVI) at 185 °C. In received hybrids, denoted $Eu(thd)_x$@MCM-41, the same maximum yield [Eu]/[Si] = 8.2 at% on average has been achieved with either methods. The molar ratio x = [thd]/[Eu] is 0.6 on average for WI samples, and 1.5 for CVI samples. In the latter, higher contents in thd compensate lower contents in silanols with respect to the former. Rationalizing the possible bonds exchanged at the silica surface leads to a great diversity of possible co-ordination schemes according to the expression $\sum[Si(OH)_{n-x}(O)_xEu(thd)_{3-x}]$ (where $\sum$ means that surface species are considered). Chromophore neutral ligands phenanthroline (phen) or bipyridine (bipy) have been added to induce efficient Eu^{3+} luminescence under 270–280 nm excitation, via the antenna effect. For the most favourable case, $(phen)_yEu(thd)_x$@MCM-41, the emission intensity at 612 nm under excitation at 270 nm is 2/3 that for the genuine heteroleptic complex $Eu(thd)_3(phen)$. Moreover the hybrid material is stable up to 440 °C.

Keywords: Hybrid materials; MCM-41; Grafting; Europium(III); Wet impregnation; Chemical vapour infiltration; Luminescence

1. Introduction

The grafting of metal complexes onto the inner walls of mesoporous silica SiMCM-41 (hereafter abbreviated MCM-41) has been widely investigated, mainly to prepare precursor compounds subsequently transformed into inorganic materials by thermal treatment, most often for the purpose of application in catalysis. Several review articles treat of surface modifications in mesoporous silica [1] and [2]. As stated by Trong On et al. [2], the fixation of metal complexes onto the inner walls of mesoporous silica can be conducted using three approaches: (i) the direct grafting by reaction with surface silanol groups; (ii) the indirect grafting consisting in the functionalization of the silanol groups with silane coupling agents followed by the anchoring of metal complexes to the surface; (iii) the ship-in-a-bottle immobilization of metal complexes. Concerning rare-earth cations derivatives, lanthanum-containing mixed oxide clusters were formed in Cs-MCM-41 by Kloetstra et al. [3]. Gerstberger et al. have investigated yttrium bulky complexes grafted into mesoporous silica [4] and [5] by surface organometallic chemistry.

Europium(III) is a widely used red-emitting cation in mineral matrices or as inorganic complexes, in the solid state and in solution. Efficient red-emission under excitation in the near UV-blue range (300–480 nm) is achieved only for some europium(III) complexes. Organic chromophore molecules often have high absorption cross-sections in this range. It has long been observed that when such molecules are bound to europium, the absorbed energy may be efficiently transferred to the cation that in turn emits in the visible, according to the so-called “antenna effect”. A plethora of organic chromophores have proved to sensitize the luminescence of lanthanide ions. The β-diketonate ligands were among the first recognized suitable sensitizers [6]. Since then, the photo-physics of luminescent lanthanide (mainly Eu^{3+} and Tb^{3+}) complexes has been systematically studied [7].

However, the poor chemical and thermal stability of as-prepared metal-organic complexes can adversely affect many applications. These drawbacks must be overcome before development of their uses. In this respect, intensive efforts are currently made to embed them into a matrix to improve thermal, mechanical or chemical resistance. For instance, bulky hybrid materials were prepared with the metal-organic complex embedded in a silicate based matrix [8] or a polymer [9]. Some works deal with embedding europium complexes into porous matrices. Mitchell-Koch et al. [10] immobilized europium complexes within porous organic polymer hosts, and obtained luminescent materials potentially suitable for chemical sensing. The immobilization of europium complexes within mesoporous silica hosts has been described in Refs. [11], [12] and [13]. For $Eu(TTA)_3$ complexes (TTA = thenoyltrifluoroacetone) [11], it is reported that the luminescence efficiency in the hybrids is about half that of the genuine complex, whereas the temperature-related quenching of the luminescence is reduced. Encapsulation of $Eu(TTA)_4C_5H_5NC_{16}H_{33}$ into surface-modified Si-MCM-41 is claimed to give efficient red emitters with a higher stability towards UV irradiation than the corresponding complex [12] and [13].

In this work, we investigate mixed systems with Eu(III) β-diketonates [$Eu(dik)_3$] as optically active guest species and mesoporous silicas MCM-41 as a host matrix. The goal was to stabilize highly luminescent organo-lanthanides complexes in mineral hosts [14], [15], [16] and [17]. Preserving the textural characteristics of the matrix (i.e. highly ordered porosity and high surface area) in the hybrids could make these materials eminently suitable for luminescent sensing applications.

The results presented here concern the direct grafting of metal complex species starting from $Eu(thd)_3$ (thd = 2,2,6,6-tetramethyl-3,5-heptanedionate). The complex was expected to react with silanol groups dangling along the pore walls, as was first reported for titanocene dichloride by Maschmeyer et al. [18]. We used two routes: wet impregnation (WI) and chemical vapour infiltration (CVI). The precursor molecule $Eu(thd)_3$ is well adapted to these two techniques since it is both soluble in organic solvents and easily sublimed. This enabled us to compare the two approaches in terms of nature and yield of grafted species, and of reaction mechanisms.

Phenanthroline (phen) and bipyridine (bipy) were used as additional ligands to tentatively improve the luminescence yield through the antenna effect. The products were characterized by chemical analyses, thermal decomposition measurements, structural and textural characterizations, and vibrational and optical luminescence spectroscopies.

2. Experimental

2.1. Samples preparations

MCM-41 silica (pore size 3.5 nm) was prepared at 115 °C in autoclave for 24 h, using the following molar ratios $1SiO_2/0.1CTAB/0.25NaOH/100H_2O$, and characterized using known procedures as described in [19] for instance. The template CTMA (cetyltrimethylammonium) was removed by calcination at 500 °C during 8 h (heating rate of 2 °C/min), and between 525 °C and 550 °C for a few hours. Template removal was checked by FTIR. $Eu(thd)_3$ was purchased from Interchim and kept in a desiccator.

MCM-41 silica destined to wet impregnation (WI) was activated under vacuum (10^{-2} Torr) at 180 °C for 4 h. Then 100 mg of activated silica was rapidly weighed and suspended in different measured volumes of a solution of $Eu(thd)_3$ (1.42×10^{-3} M) in cyclohexane, corresponding to different initial Eu/Si atomic ratios [$(Eu/Si)_i$ in Table 1]. The mixture was stirred at 25 °C for 24 h. The powder was recovered by filtration, washed several times with cyclohexane, and dried at room temperature. Hereafter and in Table 1, the samples prepared by WI are denoted W1–9. Samples W8 and W9 were intentionally not washed with cyclohexane before drying. Sample W9k was prepared in the same conditions as W9, then heated at 900 °C in air for 1 h, in order to totally calcine and remove the organic matter. A sample without europium denoted WD was obtained by impregnating silica with Hthd (0.26 moles of Hthd per SiO_2) at 25 °C until dryness.

Table 1.

Preparation and analytical data

	Preparation[a]	$(Eu/Si)_i$, at%	$(Eu/Si)_f$, at%	Ligand/Eu (molar ratio)	Analysis[a]	Proposed formula
MCM-41	Hydrated			No ligand	T	$[SiO_{1.850}(OH)_{0.30}]$, 0.86 H_2O

	Preparation[a]	$(Eu/Si)_i$, at%	$(Eu/Si)_f$, at%	Ligand/Eu (molar ratio)	Analysis[a]	Proposed formula
W1	W, O	2.1 ± 0.1	2.4 ± 0.1	0.6 thd	A	$[SiO_{1.908}(OH)_{0.242}][Eu_{0.024}(thd)_{0.014}]$
			3.3 ± 0.3		E	
W2	W, O	4.3 ± 0.2	4.7 ± 0.2	0.4 thd	A	$[SiO_{1.972}(OH)_{0.178}][Eu_{0.047}(thd)_{0.019}]$
			5.7 ± 0.5		E	
W3	W, O	6.4 ± 0.3	6.7 ± 0.3	0.4 thd	A	$[SiO_{2.024}(OH)_{0.126}][Eu_{0.067}(thd)_{0.027}]$
			7.4 ± 0.7		E	
W4	W, O	8.5 ± 0.4	8.3 ± 0.4	0.5 thd	A	$[SiO_{2.058}(OH)_{0.092}][Eu_{0.083}(thd)_{0.042}]$
			8.1 ± 0.8		E	
W5	W, O	10.7 ± 0.5	8.1 ± 0.4	0.2 thd	A	$[SiO_{2.077}(OH)_{0.073}][Eu_{0.081}(thd)_{0.016}]$
W6	W, O	12.8 ± 0.6	7.1 ± 0.3	0.6 thd	A	$[SiO_{2.020}(OH)_{0.130}][Eu_{0.071}(thd)_{0.043}]$
W7	W, O	42.9 ± 0.2	9.7 ± 0.4	0.9 thd	A	$[SiO_{2.054}(OH)_{0.096}][Eu_{0.097}(thd)_{0.087}]$
W8	W	8.5 ± 0.4	6.2 ± 0.3	1.27 (thd + Hthd)	X, T	$[SiO_{1.988}(OH)_{0.162}(Hthd)_{0.031}][Eu_{0.062}(thd)_{0.048}]$
W9	W	8.5 ± 0.4	8.4 ± 0.8	1.12 (thd + Hthd)	X, T	$[SiO_{2.032}(OH)_{0.118}(Hthd)_{0.024}][Eu_{0.084}(thd)_{0.070}]$
W9k	W, K	8.5 ± 0.4	8.4 ± 0.8	thd not analyzed	X	$SiO_{2.126}Eu_{0.084}$
S1	S, 66 h, O	8.8 ± 0.2	8.3 ± 0.4	1.6 thd	A	$[SiO_{2.016}(OH)_{0.084}][Eu_{0.083}(thd)_{0.133}]$
S2	S, 66 h	8.5 ± 0.2	9.2 ± 0.9	2.07 (thd + Hthd)	X, T	$[SiO_{2.063}(OH)_{0.037}(Hthd)_{0.084}][Eu_{0.085}(thd)_{0.092}]$
S3	S, 39 h	9.0 ± 0.2	8.1 ± 0.8	thd not analyzed	X	
S4	S, 25 h	8.6 ± 0.2	8.3 ± 0.8	thd not analyzed	X	
D1	D		7.5 ± 0.8	1.6 thd	X, C	$[SiO_{2.005}(OH)_{0.095}][Eu_{0.075}(thd)_{0.120}]$

	Preparation[a]	$(Eu/Si)_i$, at%	$(Eu/Si)_f$, at%	Ligand/Eu (molar ratio)	Analysis[a]	Proposed formula
D2	D		9.2 ± 0.9	1.7 thd	X, C	$[SiO_{2.020}(OH)_{0.080}][Eu_{0.092}(thd)_{0.156}]$
WP_1	W, 1 step	8.5 ± 0.4	5.0 ± 0.2	0.6 thd, 0.8 phen	A	$[SiO_{1.970}(OH)_{0.180}][Eu_{0.050}(thd)_{0.030}(phen)_{0.041}]$
WP_2	W, 2 steps	8.5 ± 0.4	6.6 ± 0.3	0.5 thd, 0.5 phen	A	$[SiO_{2.015}(OH)_{0.135}][Eu_{0.066}(thd)_{0.033}(phen)_{0.033}]$
WB_1	W, 1 step	8.5 ± 0.4	7.0 ± 0.3	0.5 thd, 0.3 bipy	A	$[SiO_{2.025}(OH)_{0.125}][Eu_{0.070}(thd)_{0.035}(bipy)_{0.018}]$
WB_2	W, 2 steps	8.5 ± 0.4	6.4 ± 0.3	0.3 thd, 0.2 bipy	A	$[SiO_{2.023}(OH)_{0.127}][Eu_{0.064}(thd)_{0.019}(bipy)_{0.010}]$
DP_21	D, 2 steps		6.3 ± 0.3	thd, phen not analyzed	X	
DP_22	D, 2 steps		7.0 ± 0.3	thd, phen not analyzed	X	

[a] A: Si, Eu, C, H chemical analyses (Service Central d'Analyses du CNRS); C: C, H chemical analyses (Laboratoire de Contrôle de l'ENSIACET); D: dynamical vapour phase method; E: EELS analysis; K: air calcination (900 °C); O: degassed at 150 °C/10^{-3} Torr after preparation; S: static vapour phase method, treatment duration mentioned; T: thermal gravimetric analysis; W: wet impregnation; X: EDXS analysis.

Two procedures of chemical vapour infiltration (CVI) were employed: the static vapour phase (SVP-CVI) method and the dynamic vapour phase (DVP-CVI) method, as described elsewhere in detail [16] and [17]. To prepare samples by the SVP-CVI method, weighed silica (typically 15–50 mg) and $Eu(thd)_3$ (typically 10–30 mg) were placed in two separate glass-containers open at one end (length = 25 mm, ∅ = 10 mm). The container of silica was introduced in a Pyrex-glass tube (∅ = 12 mm) subsequently linked to a vacuum pump to perform activation under vacuum (ca. 10^{-4} Torr) at 205 °C for 4 h. Then the tube was successively cooled down to room temperature under vacuum, filled with dry air, rapidly charged with the container of metal complex, linked again to the vacuum system, evacuated for five minutes, and sealed into an ampoule. The ampoule was heated at 185 °C for a period of time going from a few hours to a few days depending on the experiment. Then it was quenched in the air, to force the remaining vapour phase to condense on the glass walls, not in the powder. The containers were weighed immediately after opening the ampoule, and then kept in a desiccator. The samples prepared by the SVP-CVI method are denoted S1–4 hereafter and in Table 1.

To prepare samples by the DVP-CVI method (samples D1, 2), about 150 mg of silica were placed on a filter in the narrower part of a vertical reactor tube which could be heated by an oven as schematized in [16]. About 300 mg of the precursor was introduced in the cool part of the reactor. The silica was first activated at 205 °C under vacuum for 4 h. After cooling, still under dynamic vacuum, dry nitrogen was progressively admitted with a flow monitored at about 2 ml/min to

fluidise the silica bed. Then, the reaction temperature was raised and maintained at 185 °C. The precursor container was progressively lifted up to a zone at 150 °C so that the precursor could be sublimed. After two hours, it was lifted down to the cool part. The reactor temperature was maintained at 185 °C for another 30 min, and then let to cool down still under flowing nitrogen. Atmospheric pressure was then established by progressive admission of nitrogen.

Phenanthroline (phen) or bipyridine (bipy) were introduced as additional ligands in either one or two steps by wet impregnation (samples $WP_{1,2}$ and $WB_{1,2}$). In the two-steps method, activated silica was first impregnated with $Eu(thd)_3$. After washing and drying, 150 mg of the received powder were suspended in 150 ml of a solution of phenanthroline or bipyridine (3×10^{-3} M) in dichloromethane. One step reactions were performed by suspending 150 mg of activated silica in solutions of $Eu(thd)_3$(phen) (respectively $Eu(thd)_3$(bipy)) in dichloromethane. These complexes were synthesized in a preliminary step by reacting equimolar amounts of $Eu(thd)_3$ and phen (respectively bipy) in dichloromethane at 25 °C for 1 h, filtering, washing and drying.

Preparation of samples DP_21 and DP_22 (phenanthroline) with the vapour process was run in two steps with the dynamic vapour process: $Eu(thd)_3$ was vaporized first, and then phenanthroline.

2.2. Analyses and characterization

For most samples, the elements Si, Eu, C, H, N were analyzed by the Service Central d'Analyse du CNRS. Some C and H analyses were also performed at the Laboratoire de Contrôle at ENSIACET. The [Eu]/[Si] ratios were separately evaluated by the local probe techniques EDXS and EELS. In the latter case, the [Eu]/[Si] ratios were calculated as ([Eu]/[O]) · ([O]/[Si]), with [Eu]/[O] determined by comparison with the experimental ratio (Eu M-edge/O K-edge) in standard Eu_2O_3, and [Si]/[O] from the calculated K-edge cross-sections of silicon and oxygen.

Textural properties were characterized by N_2 sorption at liquid nitrogen temperature on samples degassed at 150°C under vacuum (10^{-3} Torr) for 12 h. N_2 sorption experiments were carried out in a Micromeritics ASAP2000 apparatus. Average pore diameters have been evaluated from the nitrogen desorption branch according to Broekhoff and De Boer [20]. This is one of the best methods to evaluate pore size of MTS materials [21]. Special care was taken in determining the BET specific area, i.e. to calculate the linearization of the BET equation by avoiding points at low pressure affected by surface heterogeneity and points at high pressure corresponding to starting pore filling. Pore volumes were calculated at the end of the step corresponding to the filling of the pores.

X-ray powder diffraction patterns were recorded on a Seifert diffractometer using CuK_α radiation.

Thermo-gravimetric and differential thermal analyses (TGA–DTA) were performed with a SETARAM LABSYS-TG apparatus, at a heating rate of 2 °C/min in oxygen flow.

Luminescence excitation and emission spectra were recorded with a Hitachi F4500 spectrofluorimeter. Luminescence spectra were also recorded with a Raman set-up (DILOR XY), equipped with a krypton–argon laser source and with an optical microscope in order to recover the spectra emitted by about 0.5–1 μm^3 of matter. IR spectra were recorded on a FT-IR Brucker Vector22. Self-supported wafers were prepared for the IR investigation and further degassed at 150 °C/10^{-2} Torr for 4 h.

3. Results

The results presented in this section will be discussed in the following section.

3.1. Samples compositions

Synthesis details and analyses results are gathered in Table 1. In the table, Wn, Sn, Dn refer to samples obtained respectively by wet impregnation (W), by the static vapour phase method (S), and by the dynamic vapour phase method (D). For mixed-ligand samples, the letters P (phenanthroline) or B (bipyridine) were added with a subscript index indicating the number of steps of preparation.

Local and overall chemical analyses of the europium content give similar results. Local probe measurements prove that europium is homogeneously dispersed in the silica matrix at the spatial resolution of the probe (150 nm). Samples W1–4 correspond to increasing initial atomic ratios $(Eu/Si)_i$. The corresponding final ratios $(Eu/Si)_f$ vary parallel to $(Eu/Si)_i$. Then a plateau is reached. The highest $(Eu/Si)_f$ ratio, as averaged from values measured for samples W4–9, S1–4, D1–2 is 8.2 at%. For the mixed-ligand samples, WP_{1-2}, WB_{1-2} and $DP_21–2$, the average $(Eu/Si)_f$ is 6.2%.

The formulas given in last column of Table 1 deserve some comments. $Eu(thd)_3$ is expected to react with silanol groups (Si–OH) dangling along the pore walls, according to the overall reaction:

$$\mathrm{SiO_{2-x}(OH)_{2x}} + z\mathrm{Eu(thd)_3} \rightarrow \mathrm{SiO_{2-x+y}(OH)_{2x-y}Eu_z(thd)_{3z-y}} + y\mathrm{Hthd}. \quad (1)$$

The coefficients z and $(3z - y)$ are deduced from the analyses. The content $2x$ in available silanol groups mainly depends on the activation process. For the samples of silica treated by wet impregnation, the value of 0.30 (3 SiOH/nm^2) was retained, according to the recent determination by Shenderovich et al. [22] from ^{15}N MAS NMR of pyridine adsorbed by samples with specific surface areas of 1010 m^2 g^{-1}. As to the samples of silica treated by either CVI methods, since they were activated at higher temperature, and since they were maintained at 185 °C during the reaction with $Eu(thd)_3$, the content in available SiOH was expected to be somewhat lower. Indeed, the value $2x$ = 0.20 (2 SiOH/nm^2) was derived from the analyses for these samples.

Reaction equation (1) postulates the transformation of $Eu(thd)_3$ into chemisorbed species through strong Si–O–Eu bonds, implying that there is no physisorbed $Eu(thd)_3$ molecules. The fact that no appreciable amounts of $Eu(thd)_3$ was just physisorbed has been attested by tentative thermodesorption experiments, comparatively with compounds prepared by reacting $Cu(thd)_2$ with MCM-41 using the SVP-CVI method [16]. When heated under vacuum at 130 °C, these compounds released about 60% of the adsorbed copper as volatile $Cu(thd)_2$. Nothing of the kind was observed for compounds prepared with $Eu(thd)_3$, even above 130 °C.

The formation of Hthd in reaction equation 1 has been proved from NMR spectroscopy of the product collected in the cold trap in DVP-CVI experiments [16]. In the DVP-CVI method, the volatile products eliminate in proportion as they form, contrarily to the SVP-CVI and the WI methods that both proceed under static conditions. It is therefore likely that at least a part of released Hthd is retained in the pores. This has been confirmed by the thermal gravimetric analyses (vide infra) on samples that had intentionally not been repeatedly washed (W8–9) and/or degassed (S2) at 150 °C/10^{-3} Torr after preparation. For these samples, the part of retained Hthd is accounted to by the term $(Hthd)_v$ in the left part of the corresponding formula in Table 1. There is no such term for samples W1–7 and S1 because any physisorbed species has been eliminated

by the repeated washings with cyclohexane and/or the degassing at 150 °C/10^{-3} Torr for the purpose of BET analysis.

Addition of neutral ligands phenanthroline or bipyridine does not modify the charge equilibrium. For these samples, the amount of neutral ligands actually fixed by europium was deduced from the content in nitrogen, and the amount of thd from the total carbon content. Hereafter, loaded samples are referred to as Eu(thd)$_x$@MCM-41, (phen)$_y$Eu(thd)$_x$@MCM-41, and (bipy)$_y$Eu(thd)$_x$@MCM-41.

3.2. N_2 sorption isotherms

The N_2 sorption isotherms recorded on loaded samples exhibit shapes characteristic of the mesoporous structure (Fig. 1). Characteristic parameters S_{BET}, V_P, D_P, and C_{BET} are gathered in Table 2. The molar ratios are extracted from the formulas given in Table 1. The parameters decrease with increasing ligand content. Sample S1, prepared by the static vapour process, exhibits lower specific area, pore volume, and pore size than samples W4–6 prepared by wet impregnation, despite comparable Eu/Si ratios.

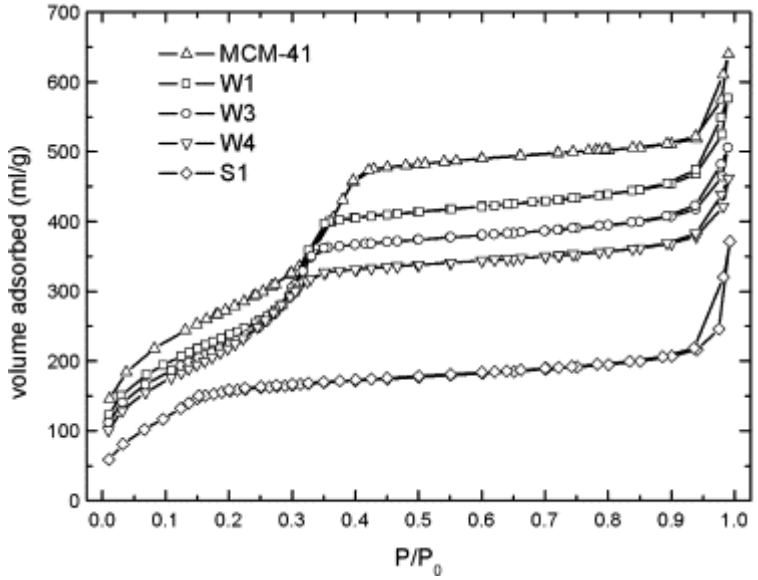

Fig. 1. Sorption isotherms of nitrogen at –196 °C.

Table 2.

Textural parameters from N_2 adsorption–desorption data and BET model (the values have been corrected in order to correspond to 1 g of SiO_2)

	Ligand/Si	C_{BET}	D_P (Å)	V_P (ml/g)	S_{BET} (m^2/g)
MCM-41	0	84	3.8 ± 0.3	0.74	1020
W1	0.014	61	3.5 ± 0.3	0.63	889
W2	0.019	45	3.4 ± 0.2	0.59	877

	Ligand/Si	C_{BET}	D_P (Å)	V_P (ml/g)	S_{BET} (m^2/g)
W3	0.027	47	3.3 ± 0.2	0.56	848
W4	0.042	35	3.2 ± 0.2	0.51	842
W5	0.016	62	3.5 ± 0.3	0.57	883
W6	0.043	56	3.6 ± 0.3	0.51	810
W7	0.087	35	3.1 ± 0.2	0.46	812
S1	0.133	26	2.3 ± 0.1	0.25	587
WP_2	0.066	45	3.2 ± 0.2	0.42	740
WB_2	0.029	60	3.3 ± 0.2	0.43	708

3.3. X-ray diffraction

X-ray diffractograms, systematically recorded in the 2θ range of 5–45°, confirmed the absence of crystallized $Eu(thd)_3$. The 2-D ordered hexagonal MCM-41 mesostructure is characterized by three peaks in the 2θ range of 1–5°. The structure is conserved upon loading by WI as well as by either CVI methods. The intensity of the peaks decreases with the content in loaded matter (Fig. 2), as expected when increasing the electronic density into the pores. The XRD pattern of W9k resulting from calcination of W9 in air at 900 °C exhibits very weak peaks of the mesostructure and no extra diffraction peaks, thus indicating a predominant amorphous state.

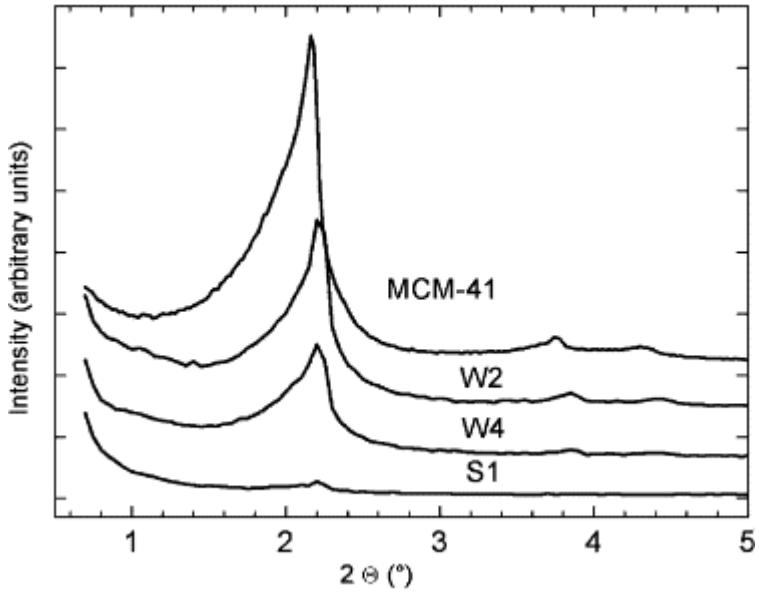

Fig. 2. X-ray diffraction patterns for pristine MCM-41 and variously loaded samples.

3.4. Thermal analyses

TGA–DTA curves recorded for WI samples after impregnation and drying (no repeated washings with cyclohexane), and SVP-CVI samples just after opening the ampoule (no degassing under vacuum), exhibit two weight losses associated with exothermic effects, as illustrated for sample W9 on Fig. 3a. The first loss is associated with a double DTA peak at 175–200 °C, and the second one with a single DTA peak at 300 ± 10 °C. Both events are assigned to the departure of organic matter. The first loss is assigned to that part of Hthd resulting from reaction (1) and retained in the pores by weak interactions. The second loss is assigned to the ligands bound to europium [15]. The assignments are based on the following observations: (i) TG and TD analyses for the sample WD that only consists of MCM-41 impregnated with Hthd (experimental part) shows an exothermic split peak at 250 °C, associated with a weight loss of 0.025 molecules of Hthd per Si atom; (ii) the curves recorded for degassed samples show no other feature than the weight loss around 300 °C, as illustrated for sample W4 on Fig. 3b. The weight loss estimated for W4 is 12% of the final mass. This fairly compares with the 10.5% calculated from the formula given in Table 1 [$SiO_{2.058}(OH)_{0.092}Eu_{0.083}(thd)_{0.042}$], assuming that the calcined product is $SiEu_{0.083}O_{2.124}$ for the sake of electroneutrality.

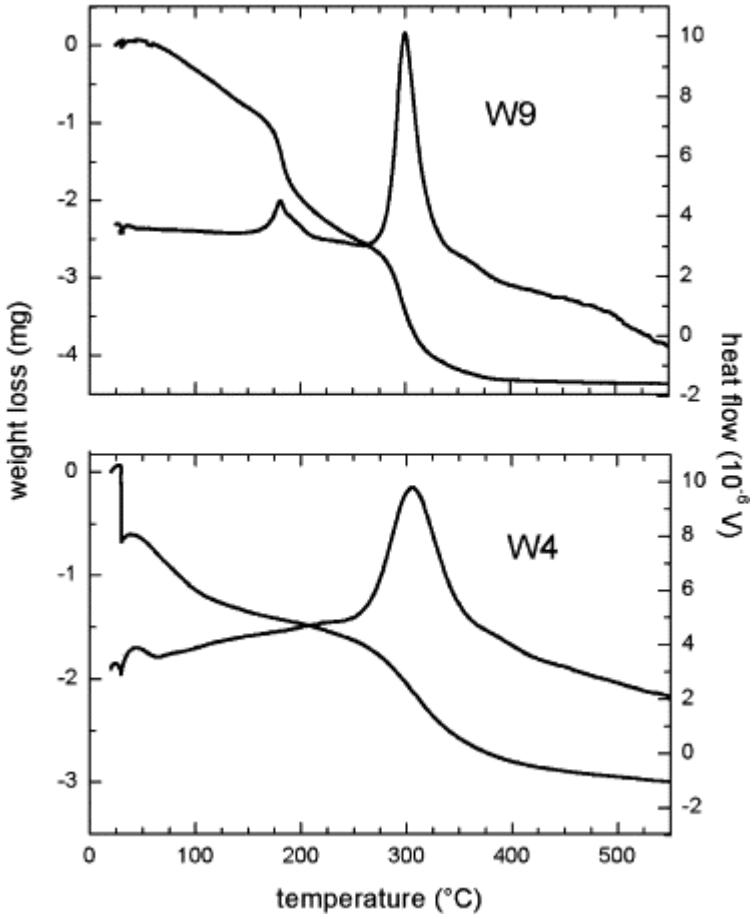

Fig. 3. TGA–DTA diagrams for wet impregnated Eu(thd)$_x$@MCM-41 hybrids, as-prepared (W9), and degassed at 150 °C/10^{-3} Torr for 12 h (W4).

Thermal analyses for the thd–phen mixed ligands samples feature a one-step decomposition at 440–450 °C. Observed weight losses with respect to final weights are 17% and 20% for WP_2 and WP_1 respectively, in agreement with those calculated from the formulas in Table 1 (17% and 18%). We may assign this unique feature to the thermal decomposition of a (phen)$_y$Eu(thd)$_x$

species, with $x \approx y \approx 0.5$. For the thd–bipy samples, two weight losses are observed at 300–310 °C and 430–440 °C. The observed overall weight loss between 150 and 550 °C is about 13% of the final weight for each sample, whereas the values deduced from the analyses are 12% for WB_1 and 6% for WB_2. The overall number of bipy ligands per europium is lower than the number of thd ligands. The thermal event at 430–440 °C is assigned to the decomposition of a species $(bipy)_yEu(thd)_x$ with $x \approx y \approx 0.2$–0.3, whereas the loss at about 305 °C is well in the range of decomposition of residual grafted $Eu(thd)_x$.

3.5. Infrared spectroscopy

Infrared absorption spectra in the energy range 1400–3900 cm^{-1} are displayed on Fig. 4. They were recorded in the transmission mode using self-supported wafers that were preliminary degassed (thermodesorbed) in situ at 150 °C/10^{-2} Torr for 4 h. The spectra were scaled using the couple of silica overtones at 1800–1900 cm^{-1}, making thus possible direct comparison of band intensities from sample to sample in the energy ranges 1400–1700 cm^{-1} ($\nu_{(OCCCO)}$), 2750–3000 cm^{-1} ($\nu_{(C–H)}$), and 3250–3750 cm^{-1} ($\nu_{(O–H)}$).

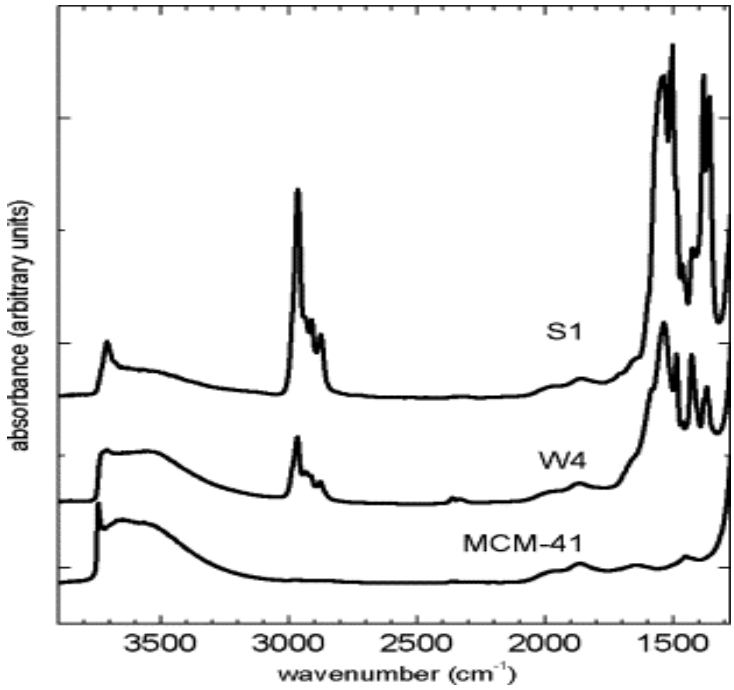

Fig. 4. IR absorption spectra recorded on self-supported wafers for unloaded MCM-41, and $Eu(thd)_x$@MCM-41 hybrids (W4, S1) after degassing at 150 °C/10^{-2} Torr for 4 h.

The intensities of the diketone $\nu_{(C–H)}$ and $\nu_{(OCCCO)}$ bands increase with the content in thd ligand, as shown by comparison of the spectra of S1 and W4 in Fig. 4. They correspond to samples with the same Eu/Si ratio. S1 is thd-rich (13.3 thd/8.3 Eu/100 Si) compared to sample W4 (4.2 thd/8.3 Eu/100 Si). The unloaded sample shows a narrow $\nu_{(O–H)}$ component at 3745 cm^{-1} that is commonly attributed to free Si–OH groups. For the heavily loaded samples W4 and S1, this component is shifted to 3710 cm^{-1}, indicating that all initially free Si–OH groups interact with grafted europium species. A broad feature at about 3500 cm^{-1} is observed for W4, and to a lesser

extent for S1.

3.6. Eu^{3+} luminescence

Eu^{3+} visible emission and excitation spectra, and visible-near-UV diffuse reflection spectra for the genuine complexes and the hybrid samples are displayed in Fig. 5 and Fig. 6.

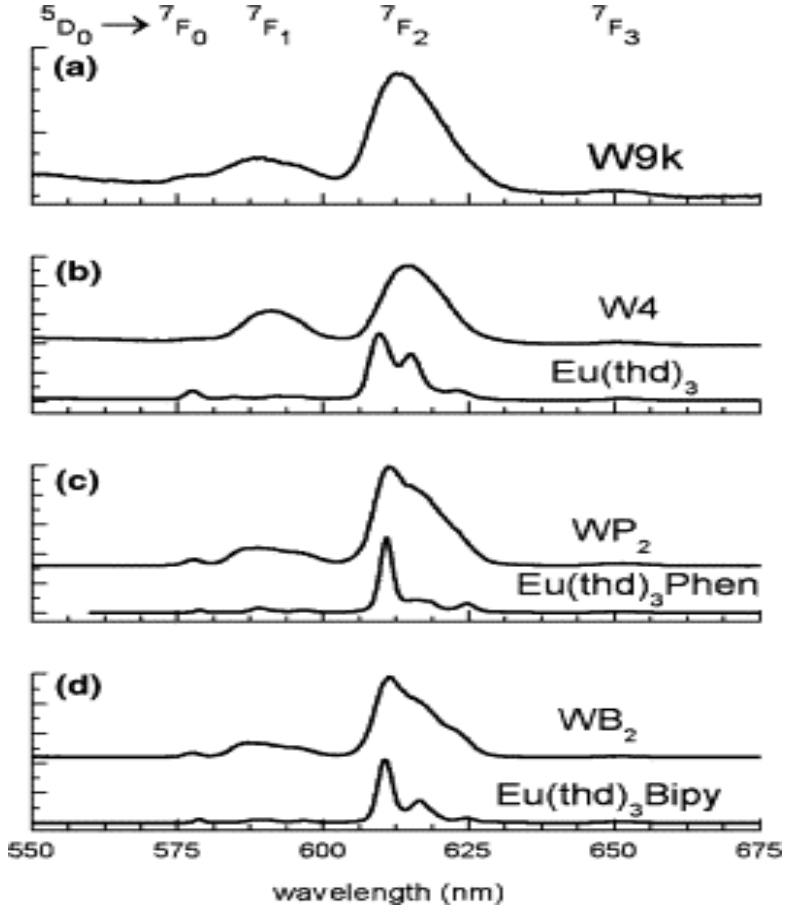

Fig. 5. Eu(III) emission spectra for (a) amorphous silica-europium oxide Eu@MCM-41 sample (W9k) and (b)–(d) upper curves, the grafted species W4, WP_2, WB_2; lower curves, the corresponding genuine complexes.

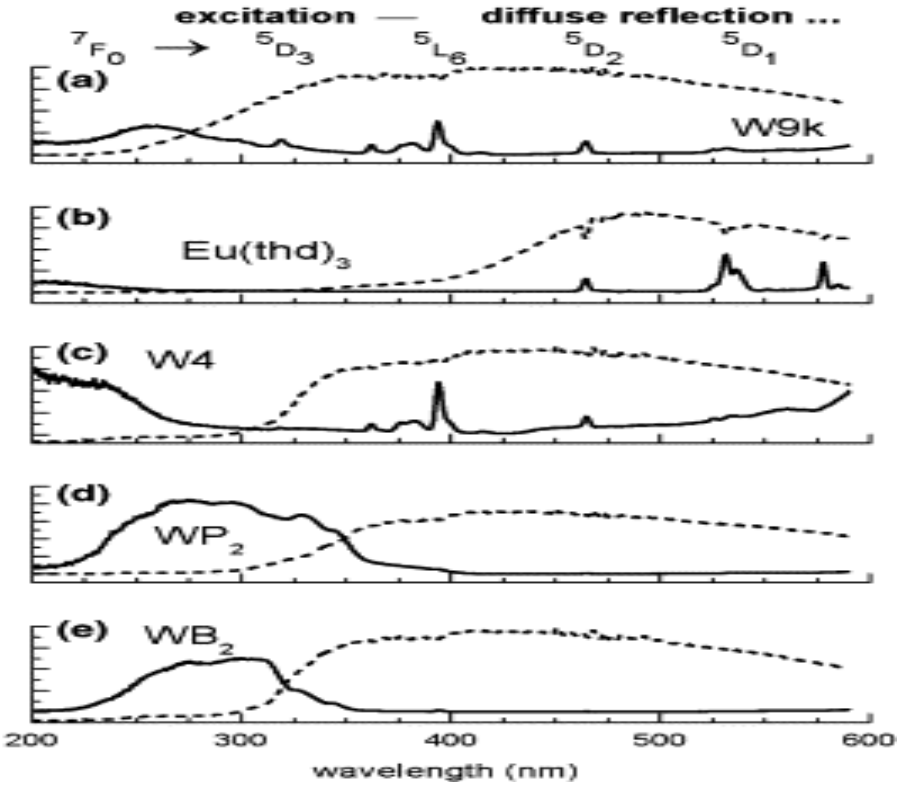

Fig. 6. Diffuse reflection spectra (dotted lines) and excitation spectra measuring the Eu(III) emission at 612 nm (solid lines) for (a) amorphous silica-europium oxide Eu@MCM-41 (W9k); (b) genuine Eu(thd)$_3$; (c)–(e) the grafted species W4, WP$_2$, WB$_2$, respectively.

Emission essentially occurs in the red part of the visible spectrum. It is unambiguously assigned to transitions between the discrete electronic levels of the 4f^6 configuration (Fig. 5). Eu(III) complexes exhibit emission spectra made of narrow lines that figure a fingerprint of the geometry of co-ordination of the cation, as shown in Fig. 5 (lower curves) by the spectra of Eu(thd)$_3$ (Fig. 5b), Eu(thd)$_3$(phen) (Fig. 5c) and Eu(thd)$_3$(bipy) (Fig. 5d). The complexes immobilized in the pores give much less structured spectra, like those reported in Fig. 5 (upper curves) for sample W4 (Fig. 5b), sample WP$_2$ (Fig. 5c), and sample WB$_2$ (Fig. 5d). The $^5D_0$–$^7F_{1,2}$ transitions are more structured, and the $^5D_0$–$^7F_0$ emission is relatively more intense for WP$_2$ or WB$_2$ than for W4.

By recording the emission with the optical microscope set-up, a volume of about 1 μm^3 is possibly analyzed to control the homogeneity of the sample with this spatial resolution. Whereas two types of emission spectra showed up for sample WB$_1$, one type only was observed for the other samples. This result means that the samples are single phases (except WB$_1$) to the scale of the probe. On the other hand, the emission lines are broader for the hybrids than for the precursor molecules in the solid state; this inhomogeneous broadening evidences that the Eu^{3+} ions adopt different local symmetries in a given single-phase hybrid.

The effect of ligands bond to Eu^{3+} shows itself on luminescence excitation spectra monitored at the main emission wavelength of 612 nm (Fig. 6). The Eu–thd interaction in Eu(thd)$_3$ is known to induce a very low-lying ligand to metal charge transfer (LMCT) state. Relaxation from this state is non-radiative [23] and [24]. The diffuse reflectance spectrum of Eu(thd)$_3$ (Fig. 6b, dotted lines)

shows strong absorption below 425 nm (absorption in the LMCT), whereas no Eu^{3+} emission is observed with excitation spectrum in this range (Fig. 6b, solid line). As shown by the dotted curves of Fig. 6, the diffuse reflection spectrum of $Eu(thd)_x$@MCM-41 (W4, Fig. 6c) exhibits an abrupt absorption edge around 325 nm, whereas the oxide Eu@MCM-41 (W9k, Fig. 6a) presents a smoother one, centred at 300 nm. Considering the luminescence excitation spectra (solid curves of Fig. 6), one observes the gradual appearance of intra-4f^n excitation lines $^7F_0$–$^5D_2$, $^5L_6$ for $Eu(thd)_x$@MCM-41 (W4, Fig. 6c), and the upper-lying $^7F_0$–$^5D_3$ transition for W9k that contains no more organic part.

Samples prepared with phenanthroline (WP_2) and bipyridine (WB_2) strongly absorb above respectively 340 nm (Fig. 6d, dotted line), and 320 nm (Fig. 6e, dotted line). Excitation at wavelengths below these values results in a strong red emission. In the excitation spectra (solid lines in Fig. 6d and e), the intra-4f transitions are much weaker than the ligand-centred absorption and even hardly visible. This evidences the antenna effect.

Samples WP_1 and WP_2, that exhibit only one thermal decomposition peak and appear homogeneous from the luminescence spectra at the microscopic scale, were submitted to further luminescence investigation. The emission intensity at 612 nm under excitation at 280 nm for the grafted species is about 2/3 that for pure $Eu(thd)_3(phen)$ in the same conditions. The $^5D_0$ emission level lifetime at room temperature is 0.80 ± 0.10 ms.

4. Discussion

Several points can be discussed: first the ability to immobilize lanthanide (Eu^{3+}) ions and organic β-diketonate(–) ligands into the pores of a MCM-41 silica matrix by the two synthesis methods employed, and the behaviour of the loaded samples versus different chemical and thermal treatments; secondly, the mechanisms of anchorage of metal-organic species onto the silica surface; and finally, the luminescence characteristics of the hybrid compounds.

$Eu(thd)_3$ was chosen as a precursor because it lends itself just as well to wet impregnation as to chemical vapour deposition. When this precursor is used without extra ligand (phenanthroline or bipyridine), both techniques give nearly the same maximum loading of inserted europium as measured by the atomic ratio $(Eu/Si)_f$. The average limit ratio determined over 12 samples (W4–9, S1–4, D1–2) is $(Eu/Si)_f$ = 8.2 at%. This corresponds to a density of 0.81 europium atoms/nm^2.

From literature data, the atomic ratio M/Si has not often been used as a measure of the metal loading in mesoporous structures. Contents are most often expressed in wt%. Table 3 gathers the metal loading ratios expressed in wt% in Refs. [2] and [3]; to convert these values in [M]/[Si] (at%) we made the assumption that the samples, analyzed after air-calcination, were mixtures of the oxides MO_n and SiO_2. For yttrium, Gerstberger et al. [5] reported an approximate loading of 0.8 Y atoms/nm^2 for hybrid compounds prepared by grafting $Y[N(SiH(CH_3)_2]_x(thf)_y$ or $Y(fod)_x(thf)_y$ on silylamide modified MCM-41, which compares rather well with the 0.81 Eu atoms/nm^2 in the present study. On the other hand, direct reaction from $Y(fod)_3$ (fod = 1,1,1,2,2,3,3-heptafluoro-7,7-dimethyl-4,6-octanedione) without preliminary silylamidation [5], resulted in half less grafted metal centers (0.4 Y atoms/nm^2). Compared with literature results, rather high metal loadings have been obtained in the present study, both by impregnation and by vapour deposition (Table 3).

Table 3.

Reported metal/silicium ratios for several metal supported MCM-41

M (MO_n)	wt%[a]	[M]/[Si] (at%)[a]	Ref.
W (WO_3)	8.2	3.0	[2]
Cr (Cr_2O_3)	2.0	2.4	[2]
Cu (Cu_2O)	10.0	9.3	[2]
Mn (MnO)	8.5	10.0	[2]
La (La_2O_3)	5.0	2.3	[3]
Y[b] (Y_2O_3)	–	8.1	[5]
Y[c] (Y_2O_3)	–	4.0	[5]
Eu (Eu_2O_3)	–	8.2	This work

[a] wt% = m(M) per 100 g sample from analysis; [M] = wt%/{M}; [Si] = (100 − {MO_n} × [Me])/{SiO_2}, { } = molar weight.

[b] From Ref. [8]: 0.8 Y/nm^2, specific area taken as 1020 m^2/g.

[c] From Ref. [8]: unsilylated route.

When bipyridine or phenanthroline are used, the final $(Eu/Si)_f$ ratio is significantly lower than 8% whatever method of preparation is used. This result seems normal when the compounds are prepared in one step because the precursor molecules $Eu(thd)_3(bipy)$ or $Eu(thd)_3(phen)$ are more encumbered than $Eu(thd)_3$. The same observation for the two-step process suggests some etching process which we did not try to elucidate.

We describe the anchoring mechanism by the reaction between silanol groups and $Eu(thd)_3$ resulting in freed Hthd and $Eu(thd)_x$ species grafted on silanolate groups following Eq. (1). The reaction is spontaneous even at room temperature as proved by the WI experiments. The two preparative methods mainly differ by the temperature, and the use of a solvent. However, they both result in grafted europium species that are chemisorbed: the Eu atoms fasten on the silica wall by iono-covalent Si–O–Eu bonds.

It is remarkable that the two preparative methods lead to similar highest metal loadings: Eu/Si = 8.2 at% (samples W4–9, S1–4, D1–2). On the other hand, the (thd/Eu) molar ratio is systematically lower for samples prepared by wet impregnation (between 0.4 and 0.9, average = 0.6) than for samples prepared from the vapour phase (mainly between 1.6 and 1.7, one at 1.1, average = 1.5). The possible state(s) and bonding(s) of the organic ligand in the hybrid materials for special synthesis conditions must be considered.

TGA experiments have proved the presence of physisorbed species that were attributed to the formation of Hthd according to reaction equation (1). When the reaction occurs at room temperature, Hthd most likely forms H-bonds with the silica walls. In the CVI preparations, reaction between Hthd molecules and silanol groups might well occur owing to the high temperature. To check this point, a sample was prepared by treating MCM-41 with Hthd at 180 °C for 80 h under vacuum. Infrared spectra for the product as received, and for the product submitted to thermodesorption under vacuum at 100 °C for 2 h, showed that not all of the adsorbed Hthd thermally desorbed. Though weak, lines characteristic of the β-diketone were still there after thermodesorption, thus confirming that some Hthd molecules are chemisorbed at high temperature. This effect concerns only a small amount of molecules compared to the total amount

of the ligands in the samples, so that we consider the CHN analyses as mainly corresponding to the ligands bound to europium.

Each $Eu(thd)_3$ molecule may react with one or a few neighbouring silanol groups, according to the scheme:

$$\sum[(SiOH)_n]+Eu(thd)_3=\sum[Si(OH)_{n-x}(O)_xEu(thd)_{3-x}]+xHthd,$$

where $\sum[(SiOH)_n]$ designates n neighbouring silanol groups on the pore surface. Let us recall that the numbers of silanol groups per nm^2 are not the same for the WI experiments and for the CVI experiments. As mentioned in Experimental Part, the silica was activated at 180 °C prior to wet impregnation and at 205 °C prior to chemical vapour infiltration. It is also reasonable to assume that dehydroxylation does continue to some extent during the reaction with $Eu(thd)_3$ in experiments carried at high temperature. For these two reasons, the number of silanol groups available for reaction is expected to be less for samples reacted with the vapour phase at 180 °C than for those treated in a solvent at room temperature. The consumption of surface silanol groups shows up on IR spectra in the energy range 3250–3750 cm^{-1}. This part of the spectra recorded for samples of W4, S1, and unloaded MCM-41, degassed at 150 °C/10^{-2} Torr for 4 h, are displayed in Fig. 4. The narrow peak at 3745 cm^{-1} in pure MCM-41 has been ascribed to non-interacting isolated silanol groups [25], [26] and [27]. It is no more observed after loading (Fig. 4, samples W4 and S1) which suggests that the Si–O–Eu bonding preferentially involves the so-called "isolated" silanols. As for the remaining OH vibrations, they can be assigned to non-deprotonated silanols possibly involved in the entrapping of guest species, as discussed below.

Before discussing the co-ordination of Eu on the pore surface, the following points must be stated. Firstly, europium is currently eight- or nine-fold co-ordinated in its metal complexes. It has a co-ordination number of 6 in the oxide Eu_2O_3. The use of encumbered ligand is a long-known strategy to reach low co-ordination numbers in co-ordination chemistry. The silanol groups dangling along pore walls in mesoporous silica may be considered are encumbered ligands because of the rigidly extended surface to which they are attached. On the other hand, thd(–) is an encumbered ligand too. On the basis of data from crystal structure [28], a $Ln(thd)_3$ molecule is inscribable in a sphere of 12–15 Å in diameter, to be compared with the pore diameter of about 35 Å. Therefore grafted europium species most likely have low co-ordination numbers. Secondly, the ligand thd(–) may co-ordinate electropositive metal centres in several ways. Besides its usual chelating mode, it may bridge two or three metal centres as observed for the tetrameric species $[Ba(thd)_2]_4$ for instance (Scheme 1) [29].

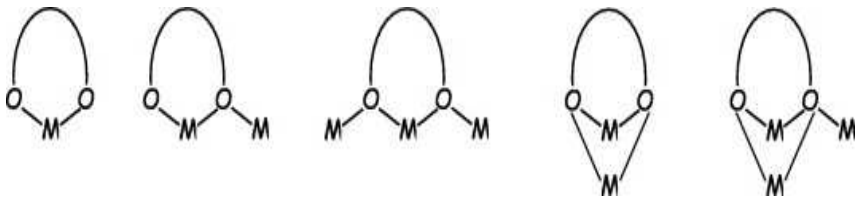

Scheme 1. The different co-ordination schemes of the ligand thd in the two known modifications of $[Ba(thd)_2]$ [29].

Several models have been proposed for the silica surface. They are discussed by Shenderovich et al. [22] who propose a model based on regular arrangements of 6-membered trydimite fragments with every second atom bearing an OH group (Q^3 Si). There are no $Si(OH)_2$ groups (Q^2 Si).

Examination of the model surface shows that most of the silanol groups are arranged like in model silsesquioxanes. Feher et al. [30] have shown that the six-member ring [–O–Si(OH)(R)–O–Si(O)(R)]$_3$ in trisilanol silsesquioxanes of general formula $R_7Si_7O_9(OH)_3$ is a good model for tridimite (0 0 0 1) and cristobalite (1 1 1) surfaces. The ability of this ring to behave as a tripodal ligand towards electropositive transition metal (Fig. 7) has been proved through crystal structure determinations such as for $[(C_5Me_5)Zr(Si_7O_{12})(c\text{-}C_6H_{11})_7]$ [31] or $[OP(Ph)_3)_2Y_2(Si_7O_{12})(c\text{-}C_5H_9)_7]_2$ [32]. This supports binding schemes between europium and the pore surface in which up to 3 neighbouring silanolate SiO^- groups on Q^3 silicon atoms may bond an europium cation. On the other hand, the silanolate group of a Q^3 silicon atom may bind to one (μ_1-SiO), two (μ_2-SiO) or three (μ_3-SiO) europium cation. Besides, silanol and siloxane groups may act as neutral co-ordinating ligands. It results a great diversity of co-ordination schemes that may coexist. In the following, we tentatively estimate the contributions of these different schemes in our samples.

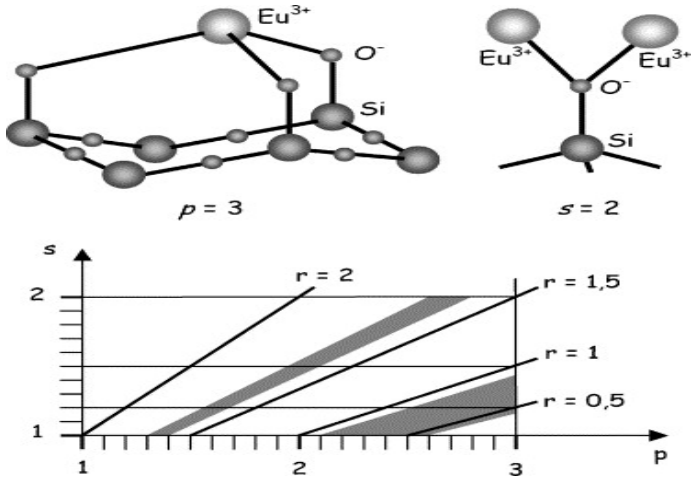

Fig. 7. Abacus showing the podality *p* versus the number *s* of Eu^{3+} cations bond to the same SiO^-, for different values of *r* = Eu/thd molar ratio. The grey zones correspond to the WI samples (right) and to CVI samples (left). The structural drawings illustrate a case of podality *p* = 3 about a tridymite fragment, and a case of *s* = 2 cations sharing the same SiO^- group.

Let *p* (podality) be the average number of Eu-OSi bonds per Eu^{3+} cation and *s* the mean number of Eu^{3+} cations per silanolate SiO^- site (Fig. 7). This leaves [3 − (*p*/*s*)] positive charges on the cation. The average number of thd(–) ligands per Eu^{3+} cation necessary to get electroneutrality is *r* = [3 − (*p*/*s*)]. Both *s* and *p* are larger than or equal to 1 by definition. The upper limit for *p* is 3 (*vide supra*), and a reasonable upper limit for *s* is 2 for steric reasons. It is also reasonable to assume that for steric reasons, the higher *r* the lower *s*. An abacus in Fig. 7 shows the variations of *p* versus *s* for stated values of *r*. It shows that for *r* less than 1, the podality *p* is larger than 2, and the range of variation for *s* is restricted to values between 1.5 and 1. This is the case for the samples prepared by WI ($0.4 < r < 0.9$, average = 0.6). Most Eu^{3+} cations are bound to 2 or to 3 silanolate groups, and the proportion of silanolate groups bridging two cations (i.e. *s*) is low. For samples prepared by CVI, the molar ratios (thd)/Eu are larger than 1 (mainly between 1.6 and 1.7, one at 1.1, average = 1.5). The abacus shows a wide field of co-ordination schemes for europium, with the podality *p* varying between $p < 1.5$ for $s = 1$ and $p > 2$ for $s = 2$. It is reasonable to assume that for steric reasons, the higher *r* the lower *s* then the lower *p*. This means that local co-ordination schemes involving a high podality are not favoured in CVI samples and that the average podality *p* is lower than in WI samples. These results are consistent with the higher

concentration in available pore silanols in the silica samples submitted to wet impregnation (ca. 3 nm^{-2}) with respect to those submitted to chemical vapour infiltration (ca. 2 nm^{-2}). Since the upper limit contents in grafted europium are similar for both approaches, the lower content in SiO^- in the latter is consistently compensated by the higher content in thd^-, for the sake of electroneutrality; and the lower overall podality *p* is consistent with the lower content in silanol groups. From the contents in grafted cations and diketonate ligands, and in initially available silanol groups, all the compounds should contain residual silanol groups. This is confirmed by the infrared spectra in the energy range 3250–3750 cm^{-1}. At least part of these residual groups probably co-ordinate europium as neutral ligands: the peak at 3710 cm^{-1} might originate in silanols forming dative bonding [SiO(H) → Eu] with europium.

The Eu^{3+} visible luminescence of $Eu(thd)_x$@MCM-41 is weak. It is observed after excitation in the discrete Eu^{3+} levels, and the lines are broader than for genuine $Eu(thd)_3$ (Fig. 5b). In agreement with all above-reported results, the Eu^{3+} emission characteristics show that the local environment of the cation is strongly modified in $Eu(thd)_x$@MCM-41 compared with $Eu(thd)_3$. Actually the emission spectrum for sample W4 resembles more that for the air-calcined sample W9k than that of genuine $Eu(thd)_3$ (Fig. 5a and b). The observation of broaden lines for W4 versus $Eu(thd)_3$ is well explained by the diversity of coexisting co-ordination schemes. The same is true for the air-calcined sample W9k, an amorphous silica-europium mixed oxide (Eu@MCM-41). The excitation spectra for the three samples (Fig. 6, solid lines) show the diminution of the luminescence quenching effect via the LMCT state when going from genuine $Eu(thd)_3$ (Fig. 6b) to grafted $Eu(thd)_x$@MCM-41 (W4, Fig. 6c), and to the amorphous oxide Eu@MCM-41 (W9k, Fig. 6a). These observations are consistent with the fact that there are less $(thd)^-$ bound to every europium cation in the grafted species than in $Eu(thd)_3$.

Studies on the encapsulation and luminescence properties of Eu(III) β-diketonates are reported in Refs. [11], [12] and [13]. These papers describe the incorporation of $Eu(TTA)_3$ (TTA = thenoyltrifluoroacetone) or $Eu(TTA)_4$(*N*-hexadecylpyridinium) in Si-MCM41, either unmodified or pre-treated with *N*-(3-trimethoxysilylethyl)ethylenediamine. In either case, the results are interpreted considering that the entire complex is encapsulated. The grafting process described in Refs. [12] and [13] is based on hydrogen bonding interactions between the ligand (TTA) and the pore walls. This is in marked contrast with our study that has evidenced the direct grafting of optically active Eu(III) species through strong iono-covalent bonds of the emitting species with the pore surface.

The europium emission spectra for samples loaded with heteroleptic species (WP_2 and WB_2, Fig. 5c and d) show some differences with respect to that of $Eu(thd)_x$@MCM-41 (W4, Fig. 5a), due to the effect of the additional ligand. Each spectrum differs from that of the corresponding precursor complex in the line broadening essentially. The effect of an additional ligand is more visible in the excitation spectra (Fig. 6d and e). The excitation centred on the chromophore absorption band, i.e. around 270 nm for phenanthroline or bipyridine, results in Eu^{3+} visible emission. This antenna effect further proves that phenanthroline as well as bipyridine does chelate europium, to give grafted species denoted $(phen)_yEu(thd)_x$@MCM-41 and $(bipy)_yEu(thd)_x$@MCM-41. All the observations made on the samples treated with phenanthroline could be interpreted from a homogeneous phase, whereas the samples treated with bipyridine proved less homogeneous in terms of chemical composition and luminescence response. For $(phen)_yEu(thd)_x$@MCM-41, the emission intensity observed at 612 nm under excitation at 280 nm is about 2/3 that for the genuine complex $Eu(thd)_3(phen)$ measured in the same conditions. The $^5D_0$ emission level lifetime at

room temperature is 0.80 ± 0.10 ms. Thus, the goal to synthesize hybrid materials with a good Eu^{3+} luminescence has been achieved with these hybrids. Moreover, the hybrids are thermally stable up to a temperature of 440–450 °C, at which the grafted species starts to decompose.

5. Conclusion

The grafting of europium(III) onto the inner walls of mesoporous silica has been achieved starting from the unmodified MCM-41 silica and from [Eu(thd)$_3$] (thd = 2,2,6,6-tetramethyl-3,5-heptanedionate), using two routes: wet impregnation (WI), and chemical vapour infiltration (CVI). Received hybrids are denoted Eu(thd)$_x$@MCM-41. The same yield expressed as (grafted Eu atom)/(silicon atoms) is achieved for both methods: [Eu]/[Si] = 8.2 at%. The molar ratio x = [thd]/[Eu] is on average 0.6 for samples prepared by WI, and 1.5 for samples prepared by CVI. In the second class of samples, the lower content in silanols is compensated by the higher content in (thd). Rationalizing the possible bonds exchanged at the silica surface leads to consider a great diversity of co-ordination schemes for the trivalent cations according to the general expression $\sum[Si(OH)_{n-x}(O)_xEu(thd)_{3-x}]$. Europium ions are bound to one, two or three silanolate $(SiO)^-$ groups and to one or two $(thd)^-$ ligands that can also bridge two or three metal centres. Two cations may also share one $(SiO)^-$. Silanol and siloxane groups may act as neutral co-ordinating ligands.

Due to its electronic scheme, the Eu(thd)$_3$ complex is not suitable to observe Eu(III) emission under excitation in the violet-near UV range. Similarly, the Eu(thd)$_x$@MCM-41 samples exhibit only a weak red luminescence, that is observed after excitation in some of the 4f electronic levels. Adding a chromophore molecule (phenanthroline, bipyridine) greatly enhances the Eu^{3+} emission when the excitation is centred on the chromophore absorption band, i.e. around 270 nm. The observation of the antenna effect proves that species (phen)$_y$Eu(thd)$_x$@MCM-41 or (bipy)$_y$Eu(thd)$_x$@MCM-41 are grafted on the silica surface following the same rules as described for Eu(thd)$_x$@MCM-41. Phenanthroline or bipyridine are neutral ligands bound to europium. For the more favourable case ((phen)$_y$Eu(thd)$_x$@MCM-41), the emission intensity observed at 612 nm under excitation at 280 nm is about 2/3 that of the heteroleptic complex Eu(thd)$_3$(phen) measured in the same conditions, a promising result for hybrid materials which are thermally stable up to 440-450 °C. Further investigations of the syntheses parameters is in progress in order to improve these properties

Acknowledgement

We thank Christine Biolley and Marie-France Driole (LMCCCO) for recording sorption–desorption N_2 isotherms; Dr. Djar Oquab (CIRIMAT) and Yolande Kihn (CEMES) for EDX analyses and Dr A. Zwick (LPST) for laser induced luminescence spectroscopy.

References

[1] K. Moller and T. Bein, *Stud. Surf. Sci. Catal.* **117** (1998), p. 53.

[2] D. Trong On, D. Desplantier-Giscard, C. Danumah and S. Kaliaguine, *Appl. Catal. A:*

General **222** (2001), p. 299.

[3] K.R. Kloetstra, M. van Laren and H. van Bekkum, *J. Chem. Soc., Faraday Trans.* **93** (1997), p. 1211.

[4] G. Gerstberger, C. Palm and R. Anwander, *Chem. Eur. J.* **5** (1999), p. 997.

[5] G. Gerstberger and R. Anwander, *Micropor. Mesopor. Mater.* **44–45** (2001), p. 303.

[6] S.I. Weissman, *J. Chem. Phys.* **10** (1942), p. 214.

[7] N. Sabbatini, M. Guardigli and J.-M. Lehn, *Coord. Chem. Rev.* **123** (1993), p. 201.

[8] A.C. Franville, Thèse d'Université, Université de Clermont-Ferrand, 1999.

[9] L.D. Carlos, V. de Zea Bermudez and R.A. Sa Ferreira, *J. Non-Cryst. Solids* **247** (1999), p. 203.

[10] J.T. Mitchell-Koch and A.S. Borovith, *Chem. Mater.* **15** (2003), p. 3490.

[11] L. Fu, H. Zhang and P. Boutinaud, *J. Mater. Sci. Technol.* **17** (2001), p. 293.

[12] L. Fu, Q. Xu, H. Zhang, L. Li, Q. Meng and R. Xu, *Mater. Sci. Eng. B* **88** (2002), p. 68.

[13] Q. Xu, L. Li, X. Li and R. Xu, *Chem. Mater.* **14** (2002), p. 549.

[14] A. Fernandes, J. Dexpert-Ghys, C. Brouca-Cabarrecq, E. Philippot, A. Gleizes, A. Galarneau and D. Brunel, *Stud. Surf. Sci. Catal.* **142** (2002), p. 1371.

[15] A. Fernandes, Thèse d'Université, Université de Toulouse (III), 2002.

A.N. Gleizes, A. Fernandes, J. Dexpert-Ghys, The Electrochemical Society Proceedings 2003-08, 2003, p. 565.

A.N. Gleizes, A. Fernandes and J. Dexpert-Ghys, *J. Alloys Compd.* **374** (2004), p. 303.

T. Maschmeyer, F. Rey, G. Sankar and J.M. Thomas, *Nature* **378** (1995), pp. 159–162.

D. Desplantier-Giscard, O. Collart, A. Galarneau, P. Van der Voort, F. Di Renzo and F. Fajula, *Stud. Surf. Sci. Catal.* **129** (2000), p. 665.

J.C.P. Broekhoff and J.H. De Boer, *J. Catal.* **10** (1968), p. 377.

A. Galarneau, D. Desplantier, R. Dutartre and F. Di Renzo, *Micropor. Mesopor. Mater.* **27** (1999), p. 297.

I.G. Shenderovich, G. Buntkowsky, A. Schreiber, E. Gedat, S. Sharif, J. Albrecht, N.J. Golubev, G.H. Findenegg and H.-H. Limbach, *J. Phys. Chem. B* **107** (2003), p. 11924.

M.T. Berry, P.S. May and H. Xu, *J. Phys. Chem.* **100** (1996), p. 9216.

Y. An, G.E. Schramm and M.T. Berry, *J. Lumin.* **97** (2002), p. 7.

J. Chen, Q. Li, R. Xu and F. Xiao, *Angew. Chem. Int. Ed. Engl.* **34** (1995), p. 2694.

A. Jentys, N.H. Pham and H. Vinek, *J. Chem. Soc., Faraday Trans.* **92** (1996), p. 3287.

A. Cauvel, D. Brunel, F. Di Renzo, E. Garrone and B. Fubini, *Langmuir* **13** (1997), p. 2773.

A. Gleizes, S. Sans-Lenain, D. Médus, N. Hovnanian, P. Miele and J.-D. Foulon, *Inorg. Chim. Acta* **209** (1993), p. 47.

A. Gleizes, A.A. Drozdov and S.I. Troyanov, *Russ. J. Coord. Chem.* **20** (1994) (12), p. 871.
A. Gleizes, S. Sans-Lenain and D. Médus, *CR Acad. Sci.* **313** (1991) (II), p. 761.

F.J. Feher, D.A. Newman and J.F. Walzer, *J. Am. Chem. Soc.* **111** (1989), p. 1741.

F.J. Feher, *J. Am. Chem. Soc.* **108** (1986), p. 3850.

W.A. Herrmann, R. Anwander, V. Dufaud and W. Scherer, *Angew. Chem. Int. Ed. Engl.* **33** (1994) (12), p. 1285.

Corresponding author. Fax: +33 5 62 88 56 78.

Original text : Elsevier.com